On The Relationship between the QBO and Tropical Deep Convection

CHRISTOPHER C. COLLIMORE

Department of Atmospheric and Oceanic Sciences, University of Wisconsin—Madison, Madison, Wisconsin

DAVID W. MARTIN

Space Science and Engineering Center, University of Wisconsin—Madison, Madison, Wisconsin

MATTHEW H. HITCHMAN AND AMIHAN HUESMANN

Department of Atmospheric and Oceanic Sciences, University of Wisconsin—Madison, Madison, Wisconsin

DUANE E. WALISER

Institute for Terrestrial and Planetary Atmospheres, State University of New York at Stony Brook, Stony Brook, New York

(Manuscript received 30 September 2002, in final form 27 January 2003)

ABSTRACT

The height and amount of tropical deep convection are examined for a correlation with the stratospheric quasi-biennial oscillation (QBO). A new 23-yr record of outgoing longwave radiation (OLR) and a corrected 17-yr record of the highly reflective cloud (HRC) index are used as measures of convection. When binned by phase of the QBO, zonal means and maps of OLR and HRC carry a QBO signal. The spatial patterns of the maps highlight the QBO signal of OLR and HRC in typically convective regions. Spectral analysis of zonal mean OLR and HRC near the equator reveals significant peaks at QBO frequencies. Rotated empirical orthogonal function (REOF) analysis is used to determine if ENSO variations of convection are aliased into the observed QBO signals. Some analyses are repeated using the OLR record after ENSO REOF modes have been removed, yielding very similar results compared to the original analyses. It appears that the QBO signal is distinct from the ENSO signal, although the relative brevity of the OLR and HRC records with respect to the ENSO cycle makes assessing the impact of ENSO difficult.

Three mechanisms that can link the QBO with deep convection are investigated: 1) the QBO modulation of tropopause height may allow convection to penetrate deeper in some years compared to other years; 2) the QBO modulation of lower-stratospheric to upper-tropospheric zonal wind shear may result in cloud tops being ''sheared off'' more in some years than in other years; 3) the QBO modulation of upper-tropospheric relative vorticity may relax dynamic constraints on cloud-top outflow and thus allow more cloud growth in some years compared to other years. Measures of these mechanisms—tropopause pressure and temperature, 50–200-hPa zonal wind shear (cross-tropopause shear), and 150-hPa vorticity, all from the NCEP reanalyses—are compared to OLR and HRC. QBO fluctuations of convection are generally well correlated with QBO fluctuations of tropopause height. In regions where these height fluctuations are relatively small, convective fluctuations are well correlated with QBO variations of cross-tropopause shear, especially during boreal summer and winter when convection is concentrated away from the equator and the largest tropopause height fluctuations. In fact, during summer the shear mechanism appears to dominate such that QBO-related convective behavior is different than during the other seasons. QBO convective behavior is uncorrelated with vorticity fluctuations near the tropopause.

A secondary component of this study is the description of a new, long-term OLR dataset. Using measurements from *Nimbus-6*, *Nimbus-7*, and the *Earth Radiation Budget Satellite* (*ERBS*), the 23-yr OLR record analyzed in this study was constructed. This record has fewer interannual biases due to satellite differences than the well-known NOAA OLR record and, therefore, is more useful for studies of interannual meteorological variations.

1. Introduction

The zonal winds associated with the quasi-biennial oscillation of the tropical stratosphere (QBO) induce anomalous meridional circulations (Fig. 1; Plumb and Bell 1982; Huesmann and Hitchman 2001). Westerly (i.e., eastward, hereafter ''west phase'') wind shear anomalies descending on the tropical tropopause induce anomalous equatorward motion that leads to subsidence and a warmer, lower tropopause (Fig. 1a). The compensating ascent in the subtropics induces tropopause temperature–height anomalies of the opposite sign, but

Corresponding author address: Christopher C. Collimore, Dept. of Atmospheric and Oceanic Sciences, University of Wisconsin—Madison, 1225 W. Dayton St., Madison, WI 53706.
E-mail: cccollim@wisc.edu

© 2003 American Meteorological Society

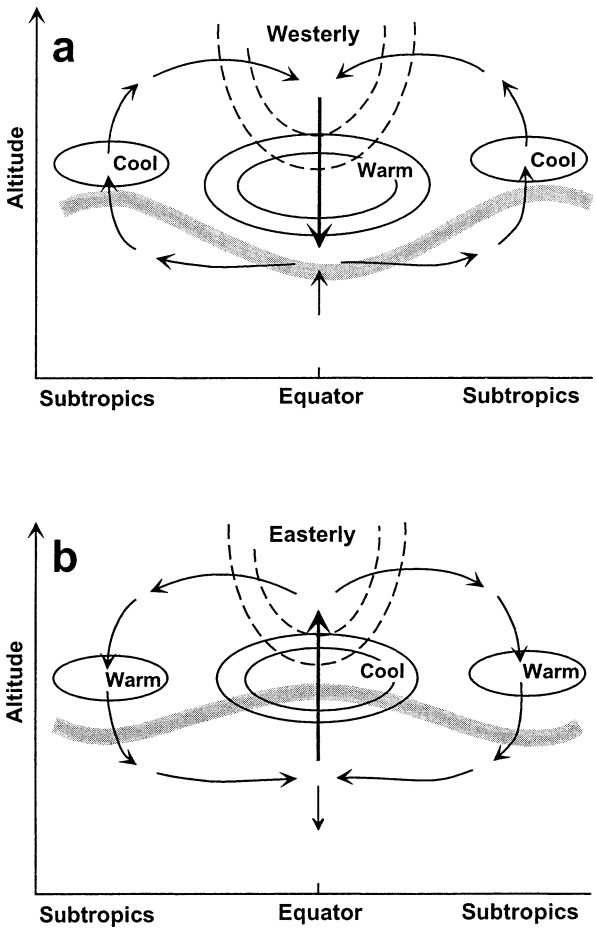

FIG. 1. Schematic representation of the mean meridional circulation driven by the QBO, after Trepte (1993). Dashed contours indicate isopleths of zonal velocity; solid contours represent anomaly isotherms. The thick, gray lines represent the tropopause. (a) Warm anomaly during descending zonal mean westerly shear; (b) cold anomaly during descending zonal mean easterly shear.

weaker in magnitude. A reverse scenario applies for the QBO east phase (westward winds; Fig. 1b). Therefore, one might expect that tropical convective clouds extending to the tropopause would be deeper during the east phase and shallower during the west phase (Gray et al. 1992; Reid and Gage 1985).

The QBO zonal winds themselves may also affect the height of convective clouds (Gray et al. 1992). Strong lower-stratospheric to upper-tropospheric wind shear may disrupt the internal coherence of convective clouds as they penetrate into the stratosphere; essentially, cloud tops may be sheared off. Weak cross-tropopause shear may allow clouds to penetrate to higher altitudes. The state of the upper-tropospheric winds at the time and location of cloud formation dictates whether the east or west phase of the QBO will produce strong shear. Given prevailing westerlies at the tropopause, for example, the east phase will induce stronger shear than will the west phase. Since upper-tropospheric winds are geographically quite variable in the Tropics, shear associated with both phases of the QBO may diminish cloud height in some locations and allow deeper than normal convection in other locations.

Huesmann and Hitchman (2001) showed that the QBO modulates upper-tropospheric winds in the Tropics. The associated vorticity variations in the upper troposphere may be yet another mechanism by which the QBO modulates deep convection. Weak absolute vorticity at cloud top is conducive to mass outflow. Less restricted outflow at cloud top is, in turn, conducive to cloud growth (Montgomery and Farrell 1993; Knox 1997; Mecikalski and Tripoli 2003). The QBO west phase can produce anticyclonic vorticity anomalies in much of the tropical upper troposphere, thus possibly enhancing the growth of convective clouds penetrating to the tropopause. A reverse argument applies to the east phase.

In general, the deeper a convective cloud is, the larger its diameter (Byers and Braham 1949; Gagin et al. 1985; Rosenfeld and Gagin 1989). Bigger convective clouds lead to more convergence of mass, moisture, and energy at low levels, which is conducive to the formation of more convective clouds (Gray et al. 1992; Mapes 1993; Knaff 1993; Ulanski and Garstang 1978). Thus, as Gray et al. noted, increased vertical extent of convection associated with the QBO should lead to greater cloud amount (i.e., greater horizontal extent and greater frequency), while decreased vertical extent should lead to lesser cloud amount. We test whether the height and amount of tropical deep convection vary with the QBO. We then test tropopause height fluctuations, cross-tropopause shear, and upper-tropospheric vorticity variations as mechanisms linking the QBO with deep convection.

2. Data

A study of this kind requires a record of tropical deep convection covering the Tropics and spanning several cycles of the QBO. Only a few records—all from satellites—meet these criteria. This section describes the satellite records chosen for this study. It also describes the records used to characterize the atmosphere in the vicinity of the tropopause and to define the El Niño–Southern Oscillation (ENSO) cycle.

a. NASA OLR

Satellite observations of outgoing longwave radiation (OLR) have long been used to measure the amount and cloud-top height of convective clouds. Because of its thickness, a convective cloud emits its upward radiation in direct relation to the temperature of its top. Therefore, for a cumulus cloud, OLR is an inverse function of cloud-top height (hereafter ''cloud height''). In general, deep convective clouds emit the lowest levels of OLR observed by satellites in the Tropics. Thus, tropical OLR

measurements below a certain threshold can be used to indicate the presence of convection.

The OLR record of the National Oceanic and Atmospheric Administration (NOAA; Gruber and Krueger 1984) has been used in a number of tropical convection studies. However, as shown by Waliser and Zhou (1997), the NOAA OLR record suffers from temporal and spatial sampling biases that may contaminate its depiction of the sort of low-frequency variability explored in this study. Data from 11 different polar-orbiting satellites were concatenated to create the 25-yr record (June 1974–February 1999). All 11 are sun-synchronous, always viewing the earth at roughly the same local time of day (the specific time of day can change from satellite to satellite). Diurnal variations in convection can result in biases between OLR observations from sun-synchronous satellites with different local overpass times. Collectively, the NOAA record satellites have six different local overpass times (the fifth and sixth of which are repeats of overpass times from earlier in the record). Moreover, the overpass times for many of the satellites changed dramatically over time due to orbital drift. Lucas et al. (2001) removed much of the satellite–overpass time bias from the NOAA OLR record using a targeted rotated empirical orthogonal function (REOF) analysis. However, the authors of that study acknowledge that the corrected record still likely contains some satellite/overpass time bias.

Working with scientists at the National Aeronautics and Space Administration (NASA), we constructed a more self-consistent OLR record using data compiled at NASA. The 23-yr ''NASA record'' consists of data from just three satellites: *Nimbus-6* (July 1975–June 1978), *Nimbus-7* (November 1978–October 1987), and the *Earth Radiation Budget Satellite* (*ERBS*; November 1984–February 1998, with August–November 1993 missing). Collectively, these satellites have just two local overpass times. *Nimbus-6* and *Nimbus-7*, both sun-synchronous, always viewed the Tropics at local noon and midnight. Over the course of a month, *ERBS*, a sun-*asynchronous* satellite, views nearly all tropical locations at nearly all local times of day. The average local time of overpass during the day is roughly noon and the average at night is roughly midnight, resulting in a good match with the Nimbus data. All three satellites had minimal orbital drift, resulting in very consistent overpass times.

All three NASA record satellites carried a wide field-of-view (WFOV) instrument that measured broadband OLR (OLR at all infrared wavelengths). The NOAA instruments, however, required estimation of broadband OLR from measurements of radiation at a specific wavelength. Moreover, the specific wavelength used by the instruments changed multiple times over the course of the record (e.g., Lucas et al. 2001; their Table 1).

Comparison between the NASA and corrected NOAA records indicates that the NASA record exhibits less satellite bias. A detailed comparison of these two datasets will be reported in a future study.

As expected, even with the high consistency of the NASA satellite sensors, some reconciliation of their data was necessary. The nearly identical orbits of *Nimbus-6* and *Nimbus-7* made reconciliation of the data from each relatively simple (Bess et al. 1989; Earth Radiation Budget Experiment Data Management System 1994). A time series of zonal mean OLR between 25°N and 25°S reveals an offset between the *Nimbus-6* values and the *Nimbus-7* values. Mean *Nimbus-7* OLR is 3.12 W m^{-2} higher than mean *Nimbus-6* OLR. Further analysis indicated that this difference appears to be a result of a simple measurement offset between the ERB instruments on board *Nimbus-6* and *Nimbus-7*. Because the *Nimbus-7* record is longer and required less correction by NASA (T. D. Bess 1997, personal communication), we corrected for the offset by adding 3.12 W m^{-2} to each *Nimbus-6* observation.

Exactly three years of overlap between the Nimbus and ERBS records greatly facilitated their reconciliation. Time series of zonal mean OLR for the Tropics are nearly identical for *Nimbus-7* and *ERBS* during the overlap. However, spatial analysis revealed systematic geographical differences. These are most likely due to the different resolutions associated with the two satellites. Because of its higher orbit, the *Nimbus-7* OLR sensor had a larger field of view (or ''footprint'') than that for the *ERBS* sensor. Therefore, *ERBS* was able to resolve semipermanent features too small in scale for *Nimbus-7* to resolve. *Nimbus-7* measured OLR from such features and OLR from surrounding features at once. Removing the geographical biases is beyond the scope of this study, but the single change in resolution contained in our OLR record, upon the transition from *Nimbus-7* to *ERBS*, should have very little effect on the type of analyses used in this study, especially those involving means over large areas.

Splicing the three records together (with *ERBS* data representing the 3-yr overlap period) yields an OLR record from July 1975 to February 1998 with two 4-month gaps (July–October 1978 and August–November 1993). Values are in the form of monthly means for each 5° × 5° latitude–longitude box between 25°N and 25°S. To remove the annual cycle, we calculated the mean OLR in each box for each calendar month; from each raw monthly value, we then subtracted the corresponding calendar-month mean, yielding an anomaly record of OLR.

Over the course of a month, nonconvective clouds (especially cirrus clouds, which are not always associated with convection in the Tropics), the earth's surface, and the clear atmosphere all can contribute to the OLR from each box. As a first-order removal of boxes that are not dominated by deep convection, only boxes with raw values less than 240 W m^{-2} are included in the spectral analysis of section 3b. An OLR flux of 240 W m^{-2} corresponds to a box-average blackbody temper-

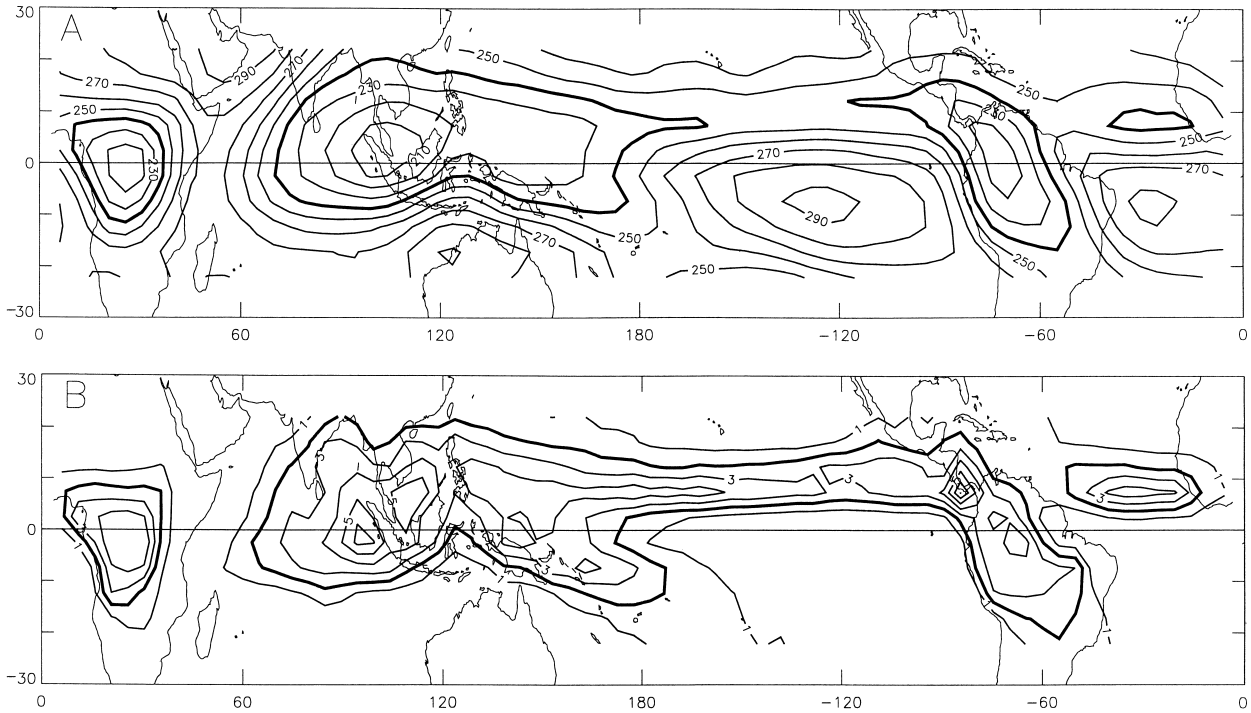

FIG. 2. (a) Mean OLR during boreal autumn (Sep–Nov); thick line represents 240 W m^{-2}. (b) Same as in (a) but mean HRC; thick line represents 2 counts month^{-1}.

ature of 255 K and a rain rate of about 210 mm month^{-1} (Wang 1994). Another filtering method we employ in other analyses is to include only values from regions dominated by deep convection over the long term. These ''chronically convective'' regions are defined as all boxes with a record-mean value, for a given calendar month, of less than 240 W m^{-2}. Thus, the number and distribution of chronically convective boxes depend on calendar month.

b. HRC

Because none of the monthly OLR values purely represent deep convection, we also analyzed the highly reflective cloud (HRC) dataset, a satellite record meant to be solely a measure of deep convection. Conceived by Kilonsky and Ramage (1976), HRC is a gridded, monthly count of cloud clusters (organized deep convection). Using visual and infrared images from NOAA or Defense Meteorological Satellite Program (DMSP) polar-orbiting satellites, for each day of the record each 1° × 1° box between 25.5°N and 25.5°S was assigned to one of two categories, cloud cluster (HRC) or not cloud cluster. HRC was subjectively identified according to cloud brightness, size, appearance, texture, cloud-top temperature, and the local cloud climatology. With allowances for variable numbers of days in a month and missing data, daily occurrence was aggregated to monthly count. The Kilonsky–Ramage record, which starts in January 1971, was extended by Garcia (1985; also see Grossman and Garcia 1990) through December 1987, resulting in a 17-yr record. Comparing it with OLR, Waliser et al. (1993) demonstrated that HRC is a superior measure of cloud cluster–scale tropical convection for many applications, especially those involving areas that are not typically deep convective.

Like the NOAA OLR, the HRC record was constructed with data from many different satellites over the years. Waliser and Zhou (1997) removed much of the resulting satellite overpass time biases from HRC, as was done with NOAA OLR. As part of their bias correction process, Waliser and Zhou remapped HRC to a 2° × 2° grid and subtracted the annual cycle. We remapped these anomalies to the 5° NASA OLR grid. All the HRC results in this study draw on the Waliser and Zhou record.

Figure 2 shows OLR and HRC averaged for all of the boreal autumn months (September, October, November) available from each record. The 240 W m^{-2} OLR contour defines the locations of the autumn chronically convective regions averaged together. The HRC contour representing 2 counts month^{-1} corresponds very well with the 240 W m^{-2} OLR contour, which is true for all seasons (not shown). All seasons considered, the only substantial difference is that HRC defines the east Pacific intertropical convergence zone (ITCZ) better than OLR, as illustrated Fig. 2. This is most likely because the ITCZ tends to be latitudinally small compared to the footprint of the instruments used to measure NASA OLR, whereas the instruments used to measure HRC

were of a high enough horizontal resolution to resolve the ITCZ. Nevertheless, we follow Collimore et al. (1998) and use OLR to define chronically convective regions. One definition for chronically convective regions facilitates OLR–HRC comparisons.

c. NCEP reanalyses

All pressure, temperature, and wind data in this study are from the National Centers for Environmental Prediction–National Center for Atmospheric Research (NCEP–NCAR) reanalyses (Kalnay et al. 1996; Kistler et al. 2001). We remapped the NCEP data to the 5° NASA OLR grid for some analyses.

Using monthly means, we constructed an index of the QBO by calculating anomalies of the 50–70-hPa zonal wind shear at each NCEP grid point on the equator and then averaging all of these anomalies. We chose 50- and 70-hPa winds to represent the QBO because the mechanisms possibly linking the QBO with deep convection that we investigate involve, for the most part, interaction between the QBO and the tropopause, and these levels are the lowest stratospheric levels available from the NCEP reanalyses. We chose a shear index instead of winds at a single level because one mechanism (tropopause height fluctuations) responds to the shear in the lower stratosphere (see section 1). See Huesmann and Hitchman (2001) for more information on the 50–70-hPa index. West phase months are classified as those with values ≥ 1.5 m s^{-1}, east phase months as those with values ≤ -1.5 m s^{-1}, and intermediate months as those with values in between. The west phase covers 106 months of the OLR record; the east phase, 93 months; intermediate periods, 65 months. For the HRC record, 91 months are west phase, 73 are east phase, and 40 are intermediate.

d. Southern Oscillation index

We use the Southern Oscillation index (SOI) as a measure of the status of ENSO. We obtained the SOI (standardized Tahiti minus Darwin sea level pressure differences) from the Climate Prediction Center's Web site (http://nic.fb4.noaa.gov/data/cddb/cddb/soi). We use 5-month running means of the SOI with values less than -0.5 to define periods of El Niño, greater than 0.5 to define periods of La Niña. Isolated values exceeding these thresholds during periods that obviously belong neither to El Niño or La Niña are not included. Similarly, three months that obviously belong to the 1996 La Niña but have values between the thresholds were assigned to that La Niña. The Climate Prediction Center's table of El Niños and La Niñas was of help in determining obvious El Niño and La Niña periods. El Niños cover 83 months of the OLR record; La Niñas, 31 months; intermediate periods, 125 months. HRC was not stratified by ENSO phase in this study.

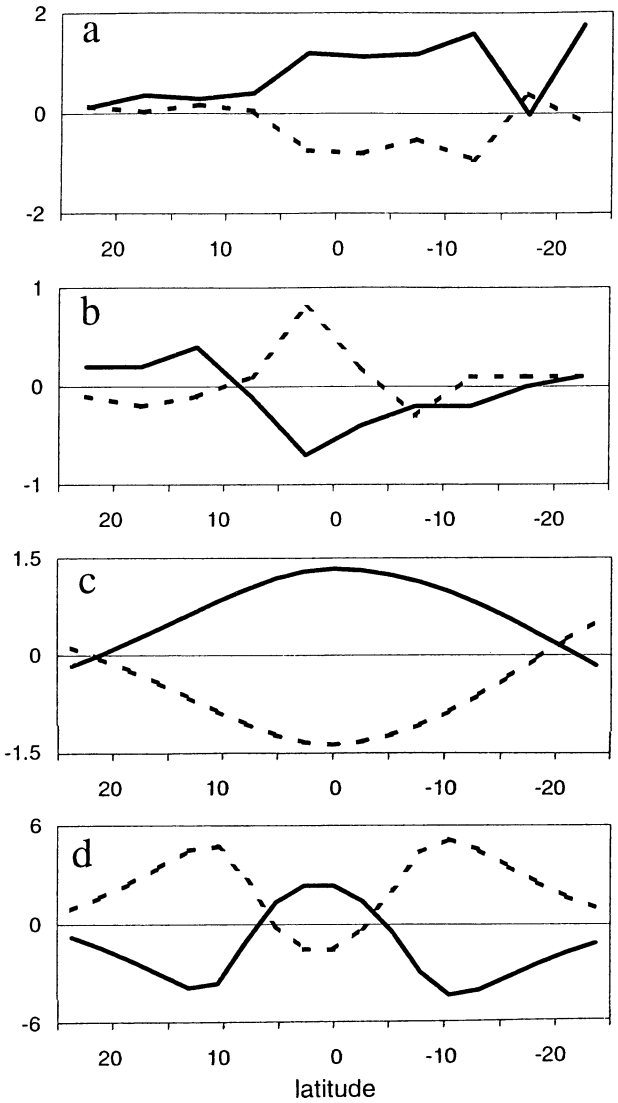

FIG. 3. Zonal mean anomalous (a) OLR in the chronically convective regions (W m^{-2}); (b) HRC (counts $\times$ 10); (c) tropopause pressure, 1958–2001 (hPa); (d) absolute values of 50–200-hPa zonal wind shear, 1958–2001 (m s^{-1}). Solid lines are for the QBO west phase; dashed lines are for the east phase.

3. Evidence of a quasi-biennial oscillation of deep convection

a. Zonal means

Zonal mean OLR anomalies averaged for the QBO west (solid) and east (dashed) phases are shown in Fig. 3a, with 5° latitudinal resolution. Only anomalies for chronically convective regions are included. Near the equator, the east phase anomalies are negative, implying deeper and/or more convection, while the west phase anomalies are positive, implying shallower and/or less convection. West and east phase magnitudes are largest between roughly 5°N and 13°S. Values are weaker and tend toward the opposite sign away from the equator.

The differences between west and east phase values are significant at the 95% level between 5°N and 5°S, using *z* scores (the nature of the variance associated with these zonal means renders Student's *t* test inappropriate). The latitudinal structure of anomalous HRC, averaged for entire latitude bands (not just the chronically convective regions), for each QBO phase roughly matches that of OLR, although the largest magnitudes are slightly skewed toward the Northern Hemisphere (Fig. 3b). The difference between west and east phase HRC values is not significant at the 95% level, using Student's *t* test, at any latitude. Figures 3c,d are discussed in section 4.

b. Spectral analysis

The OLR and HRC anomalies of Fig. 3 agree best between 5°N and 5°S, the zone where the QBO is strongest. Thus, we focus our spectral analysis on this zone. Figure 4a shows spectral analysis results for the time series of monthly mean anomalous OLR between 5°N and 5°S. Only deep convective anomalies were included in these zonal means (raw values <240 W m^{-2}), and since large anomalies result merely from the formation of convective clouds in typically nonconvective locations (as we verified during the course of our analysis), only anomalies from the chronically convective regions were included. Both 4-month gaps in the time series were filled by linearly interpolating across each gap, with the result being a time series similar to that used in Collimore et al. (1998). Spectral power is calculated with a resolution of 0.002 cycles month^{-1}, which, at QBO periods, is about 1.43 months. The spectral results reveal pronounced power at 26, 29, and 30 months. Spectral analysis of the QBO index (not shown), just for the period pertaining to the OLR record, reveals that the largest spectral peak spans 27, 29, and 30 months, with the greatest power at 27 months. The OLR peak at 30 months is comparable in power to the El Niño peaks (near 42 and 66 months) and a peak near 20 months. Tung and Yang (1994) demonstrated that interaction between quasi-biennial and annual variations should result in variability with a 20-month period. Thus, the 20-month peak may be a result of interaction between the QBO and the annual cycle of phenomena affecting OLR.

The 26-, 29-, and 30-month OLR amplitudes all exceed the 95% confidence level line. Besides testing the significance of individual amplitudes, the mean amplitude for periods throughout the QBO range (amplitudes between roughly 24 and 30 months were averaged) was tested for significance using the following Monte Carlo approach. The OLR time series was randomized and then subjected to spectral analysis. Next, the difference between the mean amplitude in the 24–30-month range and the mean of all other amplitudes was computed. This process was repeated 500 times. The difference for the original (nonrandomized) time series was computed and was larger than the difference delineating the upper 5% of the 500 ''random'' differences from the lower 95%. Thus, the mean amplitude in the 24–30-month range is significant at the 95% confidence level.

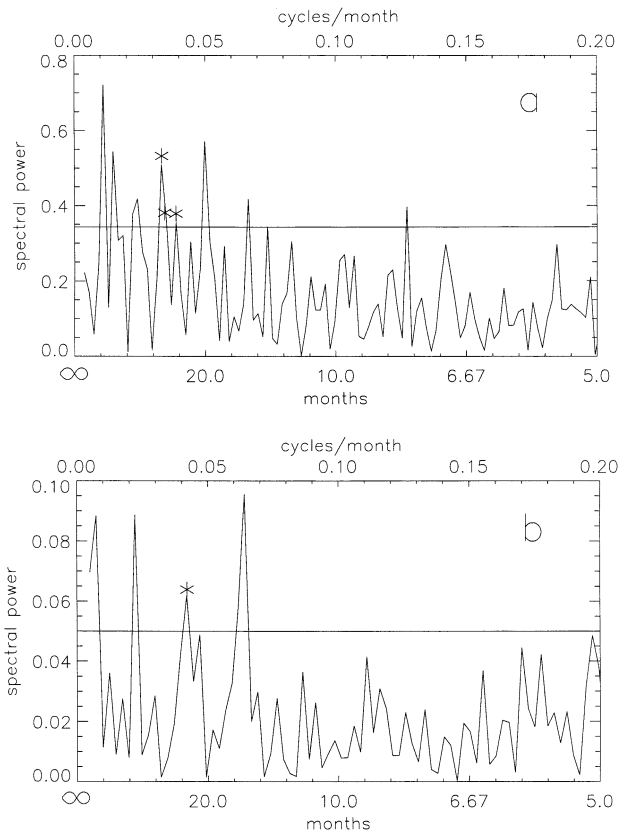

FIG. 4. (a) Spectral power of monthly mean anomalous OLR between 5°N and 5°S. Only OLR emitted by deep convection (raw values <240 W m^{-2}) in the chronically convective regions was included in the zonal means. (b) Spectral power of monthly mean anomalous HRC between 5°N and 5°S. Horizontal lines represent 95% confidence levels (the mean power for all periods plus two standard deviations). The asterisks indicate significant power at QBO periods. Power for periods less than 5 months is not shown.

For anomalous HRC between 5°N and 5°S (all longitudes), spectral power was calculated with 0.0025 cycles month^{-1} resolution—about 1.69 months at QBO periods (Fig. 4b). There is a large peak at 24 months. The largest spectral peak belonging to the QBO index for the period of the HRC record occurs at 25 months (not shown). The individual HRC peak at 24 months exceeds the 95% confidence level line and the mean HRC power between roughly 24 and 30 months is also significant at the 95% confidence level using the Monte Carlo approach. The QBO peak in Fig. 4b is smaller than the El Niño peak (near 42 months) and a large peak at 16 months. The 16-month period is very close to the period for a significant peak in the anomalous OLR power spectrum—15 months (Fig. 4a).

c. QBO difference maps

The zonal mean analyses discussed above do not take into account the longitudinal or seasonal variations of tropical convection. These variations are addressed by mapping seasonal mean HRC during the QBO west phase minus seasonal mean east phase HRC; likewise for OLR. Figure 5 shows west–east phase HRC for boreal winter (December–February), spring (March–May), summer (June–August), and autumn (September–November). Contours enveloping the chronically convective regions averaged for each season are also plotted. For the most part, winter, spring, and autumn HRC in and near the chronically convective regions and the east Pacific ITCZ indicates diminished convection during the west phase compared to the east phase (negative values), although small portions indicate enhanced convection (also see Table 1). Summer differences, however, indicate mostly increased convection over Central America and the Asian summer monsoon region during the west phase. Despite the relative brevity of the HRC record, large portions of the autumn differences in/near the chronically convective regions are significant at 95% using Student's *t* test (Fig. 6). The significant portions pass a field test at 95% confidence, with the field consisting of only the chronically convective regions (for the most part, little convection occurs, and thus no relationship with the QBO is expected outside of these regions except in the east Pacific ITCZ). As for the other seasons, only small portions of the differences in Figs. 5a–c are significant (not shown), and these portions do not pass field tests. Testing significance with *z* scores instead of Student's *t* tests produces almost identical significance maps (not shown) and field tests.

West–east phase OLR differences averaged for the chronically convective regions (Table 1) indicate convective behavior similar to that indicated by the HRC averages for each season. For the most part, seasonal maps of west–east phase OLR (Fig. 7; winter and summer not shown) are similar to those for HRC. However, the agreement is not good for some locations during certain seasons, such as the Congo region during autumn and several locations during spring. In fact, although the magnitudes differ, about half of the OLR differences are positive and about half are negative inside the chronically convective regions. OLR difference maps appear virtually the same when only the period of overlap between the OLR and HRC records is considered (July 1975–December 1987); likewise for the HRC difference maps (not shown). Because QBO variations of HRC, strictly a measure of convection, and OLR are similar to each other in the zonal means of Fig. 3, the spectral results of Fig. 4, the chronically convective averages of Table 1, and most parts of the difference maps, it seems unlikely that the disparities between the difference maps result from OLR providing a measure of convective behavior that simply conflicts with that provided by HRC. Rather, some of the other phenomena affecting OLR—cirrus clouds, the earth's surface, the clear atmosphere—probably lead to the disparities. Of the several factors influencing OLR, perhaps convective clouds have the dominant influence overall, as reflected in results that involve averages over large areas (Figs. 3 and 4 and Table 1)—but cirrus clouds or other phenomena can dominate on small scales, as reflected in those parts of Fig. 7 that conflict with corresponding parts of Fig. 5.

d. The effect of ENSO

The ENSO cycle produces well-established longitudinal shifts in tropical convection (e.g., Kyle et al. 1986; Hastenrath 1990; Wallace et al. 1998; Curtis and Adler 2000). Are the QBO signals in OLR and HRC presented above just manifestations of ENSO-induced changes in convection? Because of the length of the ENSO cycle (the period is 4–5 yr), we concentrate our ENSO analysis on OLR, the longer of our two convective indices. Mean El Niño OLR minus mean La Niña OLR differences for autumn are negative in the central and east Pacific and positive near Indonesia (Fig. 8b), similar to QBO west–east phase differences in these regions for autumn (Fig. 7b). However, the positive/negative dipole of the QBO difference map is situated about 30° longitude east relative to the dipole in the ENSO map. Elsewhere, QBO and ENSO difference patterns are dissimilar. A similar relationship holds true for QBO and ENSO winter differences (not shown). In summer (not shown) and spring (Figs. 7a, 8a), QBO and ENSO differences are pervasively dissimilar.

Despite the many discrepancies between the QBO and ENSO difference maps, there are enough similarities to suggest that, during the OLR record, El Niños may have been slightly more prominent in the QBO west phase, aliasing the QBO maps accordingly. But for the period corresponding to the OLR record, the mean SOI during the QBO west phase, -0.34, is less negative than the mean east phase SOI, -0.64. More importantly, the difference between west phase and east phase SOI is not significant at the 95% confidence level (using Student's *t* test). Neither west nor east phase mean SOI represents a significant departure (at the 95% confidence level using Student's *t* test) from -0.44, the mean SOI during the entire OLR record (in comparison, the range and standard deviation of the SOI for this period are 7.0 and 1.15, respectively). The insignificant difference between west phase and east phase mean SOI suggests that the ENSO influence on convection is roughly equal in each phase and the few similarities between the QBO and ENSO difference maps are by chance. However, as Fig. 9 shows, the frequency distribution of SOI values within each phase is different. In the east phase, SOI values are bunched in the weak–moderate range and slightly skewed toward the negative. West phase values are spread out over a greater range with a sharp peak at zero. The different SOI frequency distributions could conceivably result in different ENSO influences on con-

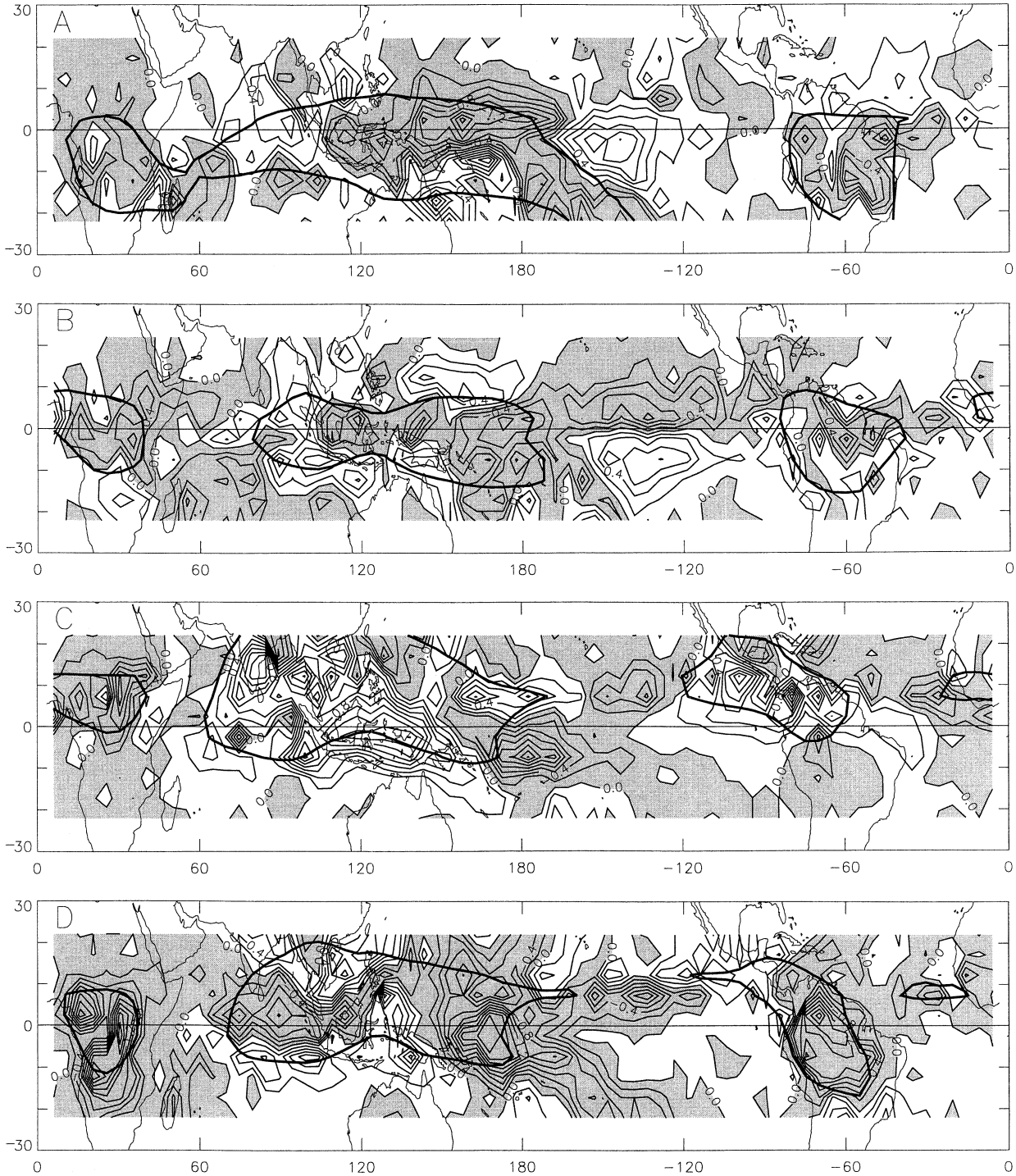

FIG. 5. (a) Mean winter (Dec–Feb) HRC during the QBO west phase minus mean winter HRC during the east phase (counts month^{-1}); (b) same as in (a) but for spring (Mar–May); (c) same as in (a) but for summer (Jun–Aug); (d) same as in (a) but for autumn (Sep–Nov). Dark lines envelop regions typically occupied by deep convection (regions where the seasonal mean value of OLR is less than 240 W m^{-2}).

vection during one QBO phase compared to the other. Thus further examination is required.

To further examine the possibility that ENSO corrupts the evidence for a convective QBO signal presented above, we performed an REOF analysis on the OLR record and identified the ENSO modes (e.g., Chelliah and Arkin 1992; Waliser and Zhou 1997). We then reconstructed the OLR record by combining all of the

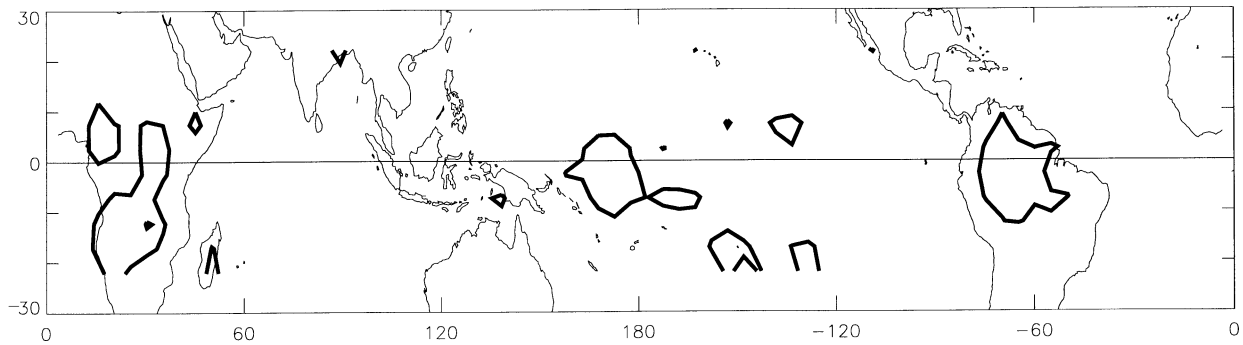

FIG. 6. Student's t values for QBO west–east phase HRC during autumn (Sep–Nov) that correspond to the 95% confidence level.

modes back together, except for the ENSO modes. Finally, we mapped QBO west–east phase differences computed from this ''no-ENSO'' OLR for comparison with the differences computed from the original OLR. The no-ENSO OLR spring differences (Fig. 10a) are very similar to the original OLR spring differences (Fig. 7a). The main discrepancy is that the Indonesian values are slightly more positive and the central Pacific values are slightly more negative for the no-ENSO OLR differences, suggesting that ENSO accounts for a portion of the original OLR differences (with La Niña conditions having slightly more impact during the west phase). The OLR/no-ENSO OLR discrepancies for autumn are also very small, but the no-ENSO OLR differences are more negative in the west Pacific and more positive in the east Pacific (Figs. 7b, 10b). Winter OLR/no-ENSO OLR discrepancies are like those for autumn except the Pacific discrepancies are more pronounced (not shown). The summer difference maps for both types of OLR are nearly identical in regard to both the patterns and the magnitudes (not shown). The spatial correlations between these seasonal OLR and no-ENSO OLR maps are high, with the minimum correlation belonging to the winter maps and the maximum belonging to the summer maps (Table 2). During the OLR record, almost all El Niños peaked during winter and were weakest during summer. Thus, one would expect the OLR and no-ENSO OLR winter difference maps to be the most dissimilar. The overall similarity between the OLR and no-ENSO OLR maps suggest that ENSO biasing of QBO west–east phase convective patterns is weak.

Caution is warranted when interpreting the no-ENSO OLR results. Due to the length of the ENSO cycle—only nine ENSO events occurred during the OLR record—a longer record is required to define truly reliable ENSO REOF modes. Thus, the ENSO signal may not have been completely subtracted from the no-ENSO OLR. On the other hand, considering there are some similarities between the spatial patterns that result from partitioning OLR by the QBO and by ENSO (Figs. 7, 8), when we subtracted the ENSO REOF modes from the OLR record we also may have subtracted some of the QBO mode. Therefore, some of the discrepancies in the Pacific between OLR and no-ENSO OLR west–east phase differences may, ironically, be due to the possibility that the no-ENSO OLR is missing some of the QBO signal.

Taken together, the three ENSO analyses (comparison of the QBO and ENSO difference maps, the significance tests of west and east phase mean SOI, and comparison of OLR and no-ENSO OLR difference maps) suggest that the QBO signal in tropical deep convection is most likely distinct from the ENSO signal. ENSO appears to modestly alter QBO west–east phase convective patterns, but this alteration is mainly confined to the Pacific and winter.

TABLE 1. Mean QBO west phase minus mean east phase OLR and HRC in the chronically convective regions. No values are significant at the 95% level using z scores.

Season	OLR (W m^{-2})	HRC (counts month^{-1})
Winter	2.42	−0.201
Spring	0.75	−0.033
Summer	−0.06	0.273
Autumn	1.47	−0.363

4. Discussion of possible mechanisms linking the QBO to deep convection

As discussed in section 1, tropopause height–temperature variations, cross-tropopause shear variations, and upper-tropospheric vorticity variations induced by the QBO may modulate the height and amount of deep convection. As predicted by theory, the zonal mean tropopause is higher than normal (lower pressure) near the equator and slightly lower than normal in the subtropics during the east phase (Fig. 3c; also see Huesmann and Hitchman 2001; Randel et al. 2000). The opposite latitudinal pattern accompanies the west phase. From 13.75°N to 13.75°S, the differences between west and east phase values are significant at the 95% level, using Student's t test. These height anomalies are generally consistent with the zonal mean convective anomalies in Figs. 3a,b: deeper and/or more convection near the equator in the east phase, shallower/less convection in the

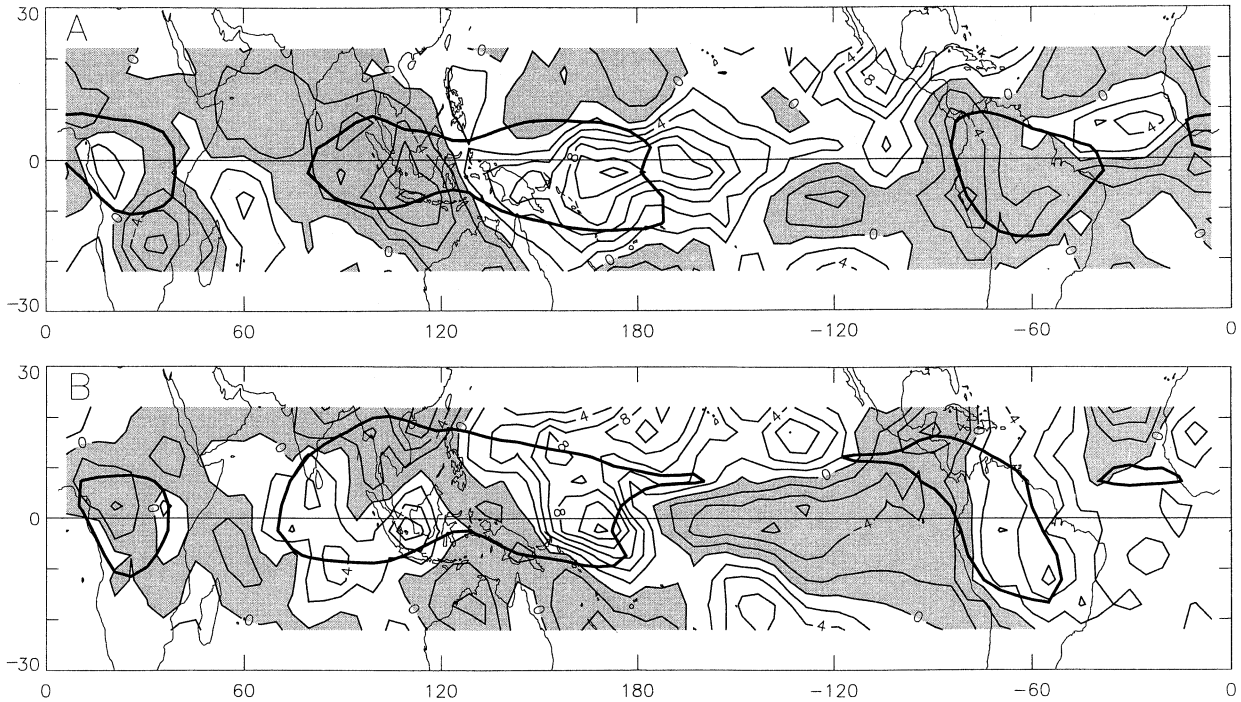

FIG. 7. Same as in Fig. 5 but for OLR: (a) spring, (b) autumn. Units are W m^{-2}.

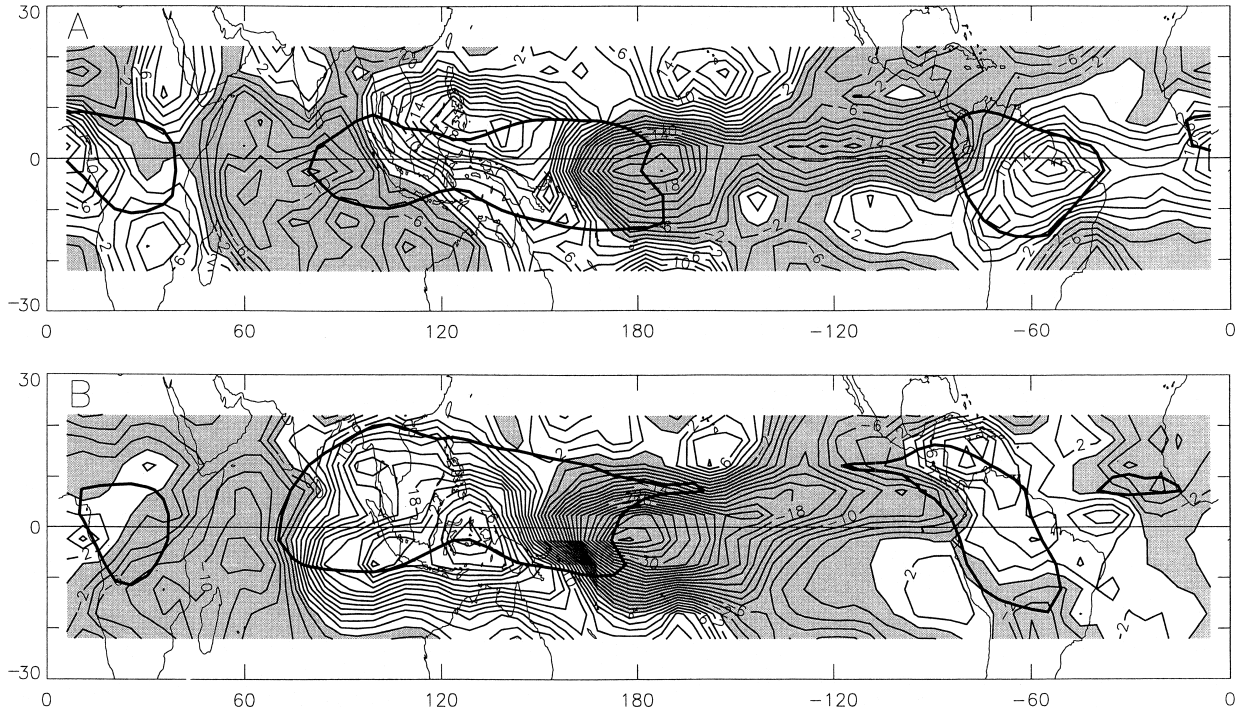

FIG. 8. (a) Mean spring OLR (Mar–May) during El Niño minus mean spring OLR during La Niña (W m^{-2}); (b) same as in (a) but for autumn (Sep–Nov). Dark lines envelop regions typically occupied by deep convection (regions where the seasonal mean value of OLR is less than 240 W m^{-2}).

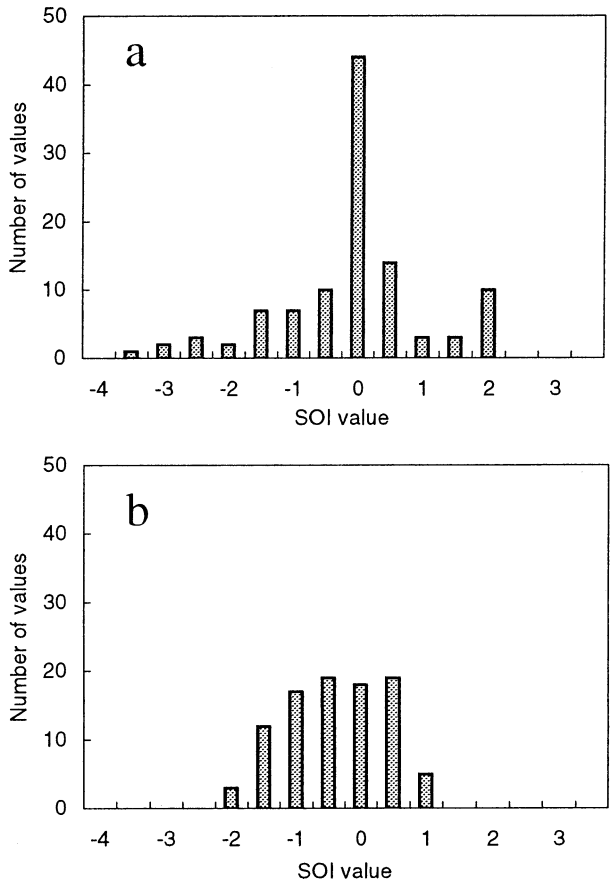

FIG. 9. Histogram of monthly SOI values, after applying 5-month running means, during the QBO (a) west phase and (b) east phase. Only SOI values during the period of the OLR record is included.

west; a slight tendency toward shallower/less convection off the equator in the east phase, deeper/more convection in the west.

The latitudinal structure of zonal mean cross-tropopause shear for each QBO phase is also similar to that for the convective anomalies, especially the HRC anomalies (Figs. 3a,b,d). The curves in Fig. 3d were derived by computing the monthly absolute value of the 50–200-hPa zonal wind shear for each 2.5° box in the Tropics, subtracting the annual cycle (which was calculated from the absolute values), then making zonal means for each QBO phase. The difference between west and east phase shear is significant at the 95% level at all latitudes except for the 2.5° bands centered on 25°N and on 5°S. The importance of upper-tropospheric winds in creating the 50–200-hPa shear can be seen by comparing Fig. 3d with Fig. 9b from Huesmann and Hitchman (2001), a similar figure but just for lower-stratospheric winds (to see the importance on a regional scale, cf. our Fig. 12 later with their Fig. 8). The zonal means near the equator indicate decreased shear during the east phase (which is favorable for convection) and increased shear during the west phase. Off the equator, shear is increased during the east phase, decreased during the west. However, the off-equator shear anomalies are larger in magnitude than the near-equator anomalies, while the opposite is true with the convection anomalies. From all four panels in Fig. 3, tropopause height and cross-tropopause shear variations appear to complement each other near the equator but oppose each other away from the equator, in terms of possible influences on deep convection.

The QBO influences tropical winds at least as low as 150 hPa (Huesmann and Hitchman 2001), thereby influencing 150-hPa vorticity in the Tropics as well. Much of the outflow from tropical convection typically occurs at 150 hPa. Therefore, we analyzed zonal means of anomalous 150-hPa vorticity (calculated from NCEP winds) during each phase of the QBO. The structures of the convective and 150-hPa vorticity (not shown) anomalies are quite dissimilar.

How do regional QBO variations of convection compare to those associated with the tropopause height, shear, and vorticity mechanisms? Since, as discussed in section 3c, cirrus clouds or other phenomena may obscure the QBO convective signal in OLR in some regions, we focus on HRC. QBO west–east phase tropopause temperatures (Fig. 11) are physically consistent with the HRC difference fields in Fig. 5. The tropopause is warmer and lower over the chronically convective regions during the west phase, and these regions generally experience diminished west phase convection, although this does not hold true for summer HRC near Indonesia and Central America. The spatial patterns of west–east phase temperature and HRC in/near the chronically convective regions usually show strong similarities. For example, negative temperature differences penetrate into the spring South American convective region from the north and south, leaving a narrow band of positive differences; negative HRC differences for this region during spring are also ''pinched'' latitudinally. Another example is the temperature bull's-eye over the western Congo convective region during autumn and the strong positive values south of this region; the HRC differences also show a bull's-eye over the western Congo and strong negative differences south of this region. West–east phase tropopause pressure differences can be close to 3 hPa in some regions, which, at the 100-hPa level, is approximately equal to 300 m of altitude difference. Thus, convection can be about 2% deeper during the east phase compared to the west phase in some parts of the Tropics.

West–east phase tropopause pressure and temperature averaged over the chronically convective regions support west–east phase convective values for these regions under the QBO influence hypothesis (cf. Tables 1 and 3). The HRC and OLR differences indicate that east phase convection is most enhanced compared to west phase convection during autumn and winter, with a lesser difference in spring. The weighted pressure and temperature differences indicate that the east phase tropo-

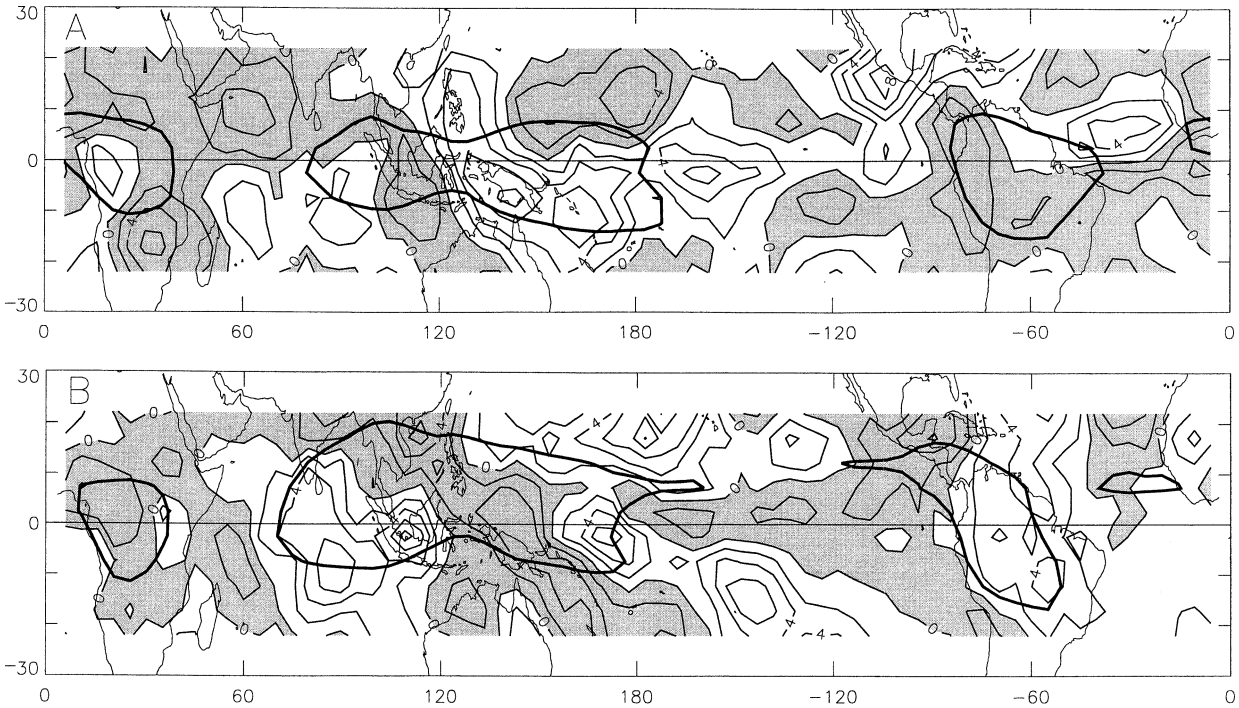

FIG. 10. Same as in Fig. 5 but for no-ENSO OLR: (a) spring, (b) autumn. Units are W m^{-2}.

pause is highest and coolest compared to the west phase tropopause during autumn and winter, with a lesser difference in spring. Summer convection is enhanced in the west phase, and the summer pressure difference, although indicative of a lower tropopause in the west phase, is the weakest of the seasonal pressure differences. The summer temperature difference, however, is slightly larger than that for spring.

Cross-tropopause shear averaged over the chronically convective regions is strong during the west phase compared to the east phase, physically consistent with the west–east phase convective differences for winter, spring, and autumn (Tables 1, 3). However, the weighted shear differences are smaller than those for tropopause pressure and temperature. Moreover, the seasonal rank of the magnitudes of the weighted shear differences does not correspond with the seasonal rank of the convective differences (shear rank: spring, summer, autumn, then winter). The spatial patterns of west–east phase convection and shear are physically consistent in many places: increased convection is associated with weaker shear, decreased convection with stronger shear (Figs. 5, 12). But in apparently just as many other places, the shear–convection relationship is physically inconsistent. So, regional QBO convective variations correspond better with tropopause height patterns than with cross-tropopause shear patterns. However, shear may play an important role in certain regions, especially during summer and winter, as discussed below.

TABLE 2. Spatial correlation coefficients between maps of mean QBO west phase minus mean east phase OLR and west phase minus east phase no-ENSO OLR. Both maps are for 25°N–25°S.

Season	r
Winter	0.76
Spring	0.82
Summer	0.97
Autumn	0.83

No clear relationship is evident between the convective difference fields of Fig. 5 and west–east phase 150-hPa vorticity difference fields (not shown). Furthermore, the weighted means of west–east phase vorticity over the chronically convective regions are about an order of magnitude smaller than the weighted means for tropopause pressure and temperature (Table 3).

Modulation of deep convection by the QBO through tropopause height fluctuations would explain why regional west–east phase HRC differences show similar values in the equinox seasons and winter but not summer (Fig. 5, Table 1). During the equinox seasons, deep convection is concentrated near the equator where the QBO and its modulation of tropopause height are strongest (Figs. 11b,d). During winter, convection is displaced to the south, but the QBO has a strong influence on winter tropopause height at latitudes well south of the equator (Fig. 11a). Most summer convection is displaced north of the equator, but summer QBO modulation of tropopause height is weak off the equator (and near the equator over Indonesia, where there is also convection; Fig. 11c). Thus, the QBO has a relatively strong influ-

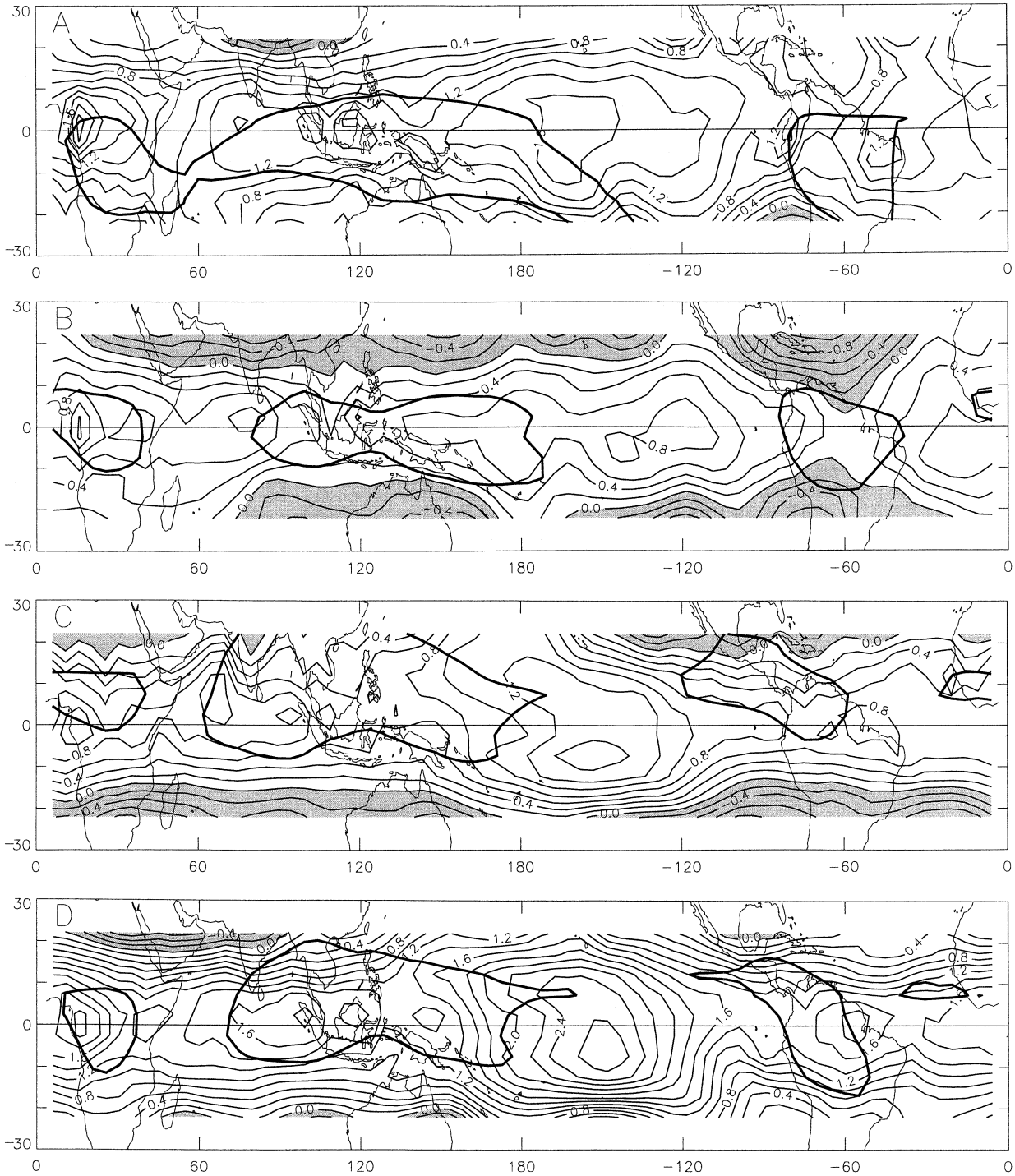

FIG. 11. Same as in Fig. 5 but for tropopause temperature: (a) winter, (b) spring, (c) summer, (d) autumn. Only years corresponding to the HRC record are considered. Units are °C.

ence on the height of the tropopause over deep convection in all seasons except summer. But instead of a QBO signal that is similar to but weaker than that for the other seasons, there is a west phase enhancement (east phase reduction) of most summer convection, evident near Central America and Indonesia. QBO variations of cross-tropopause shear could explain much of this. Near Central America and over much of the Indonesian region, the summer QBO influence on tropopause height is weak while the west phase shear is

TABLE 3. QBO west phase minus east phase difference in tropopause pressure, tropopause temperature, absolute value of 50–200-hPa zonal wind shear, and 150-hPa relative vorticity. Only data over the chronically convective regions and during the period of the HRC record (Jan 1971–Dec 1987) were considered. Weighted differences were calculated by dividing the mean for each phase and season by the corresponding standard deviation, then subtracting the east phase value from the west phase value (and so are unitless). The vorticity values have been normalized by 2Ω, the value of the planetary vorticity at the North Pole. All values are significant at the 95% level using z scores except winter shear, and spring and summer vorticity.

	Difference				Weighted difference			
Season	Pressure (hPa)	Temperature (K)	Shear (m s^{-1})	Vorticity [%(2Ω)]	Pressure	Temperature	Shear	Vorticity
Winter	3.31	1.12	0.17	0.744	1.40	0.94	0.03	0.180
Spring	1.33	0.44	2.81	−0.125	0.79	0.49	0.59	−0.047
Summer	1.20	0.66	2.64	0.073	0.57	0.64	0.54	0.028
Autumn	2.94	1.44	1.36	0.440	1.41	1.72	0.26	0.151

favorable for deep convection compared to shear for the east phase (Figs. 11c, 12b). A weak QBO influence on tropopause height combined with favorable west phase shear could also explain some of the increased west phase convection in other seasons, such as that near northern Australia in winter (Figs. 5a, 11a, 12a). The possibility of the QBO, with its quasi-biennial period, affecting tropical convection consistently (for the most part) three-fourths of the year and having a mostly reverse effect the other fourth of the year presents interesting implications for temporal variability in the troposphere.

Mapped in Fig. 13a are the correlation coefficients for anomalous HRC during each winter month of the HRC record versus the corresponding anomalous tropopause pressure. Coefficients are mostly negative where HRC in and near the chronically convective regions is lower during the west phase, reflecting elevated tropopause levels coincident with enhanced convection, lower levels coincident with reduced convection (cf. Figs. 5a, 13a). Values can exceed −0.6. Qualitatively, the spatial correspondence between the correlation patterns and the HRC patterns is poor for some places and seasons, but exceptionally good for other places and seasons, such as South America, the east Pacific ITCZ and the South Pacific convergence zone during winter (Figs. 5a, 13a), the Congo Basin during autumn (coefficients not shown), and the spring east Pacific ITCZ (coefficients not shown). The low correlations in evidence for some places and seasons are not surprising considering the many factors influencing both convective activity and tropopause height (no attempt was

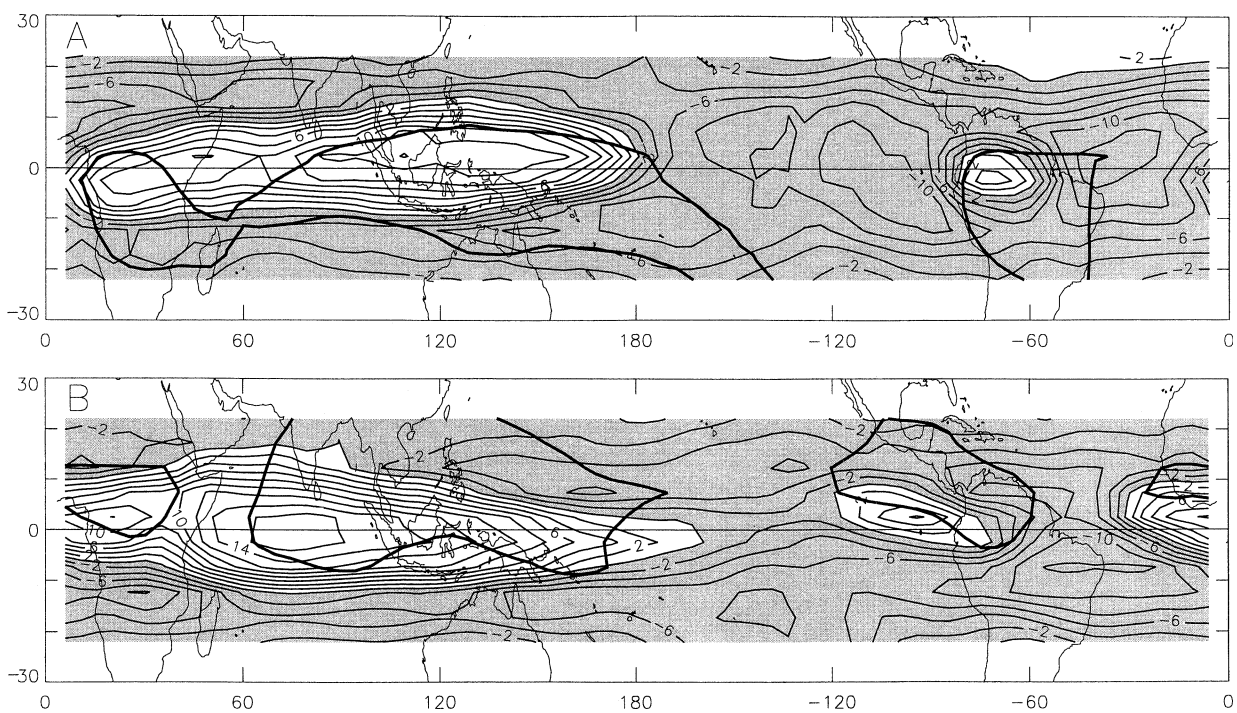

FIG. 12. Same as in Fig. 5 but for absolute values of 50–200-hPa zonal wind shear: (a) winter, (b) summer. Only years corresponding to the HRC record are considered. Units are m s^{-1}.

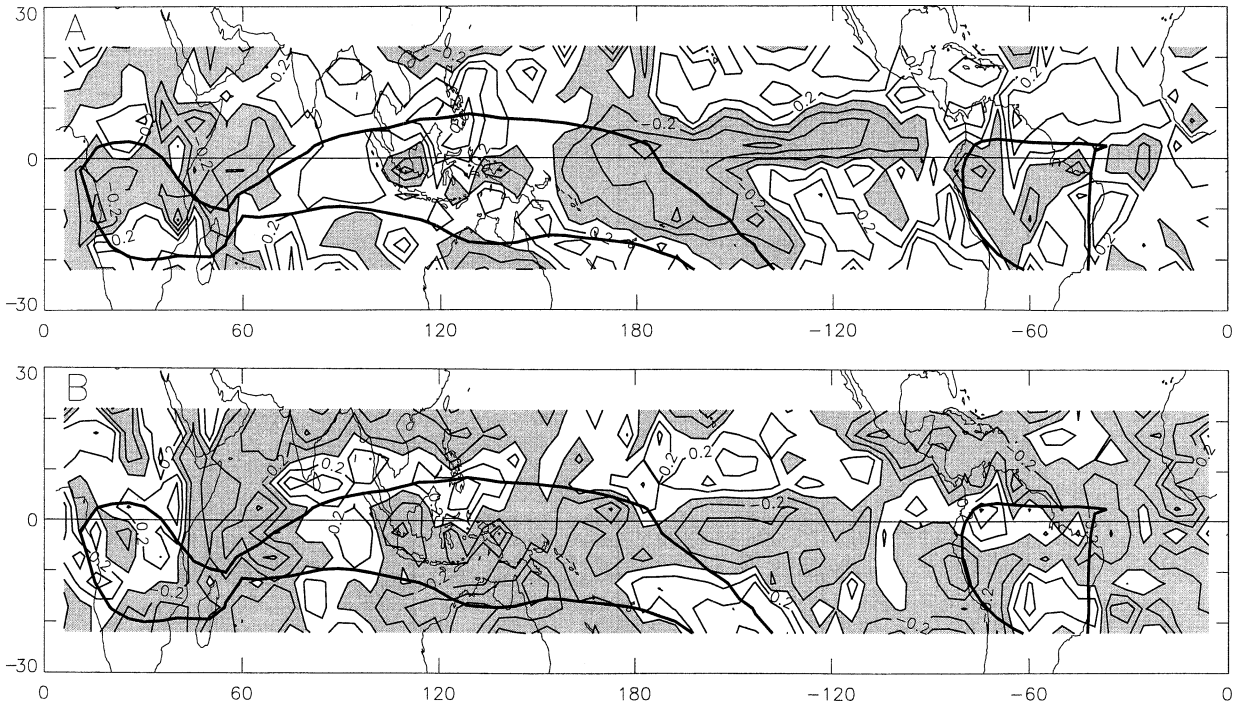

FIG. 13. (a) Correlation coefficients between monthly means of anomalous HRC and anomalous tropopause pressure during winter (Dec–Feb); (b) same as in (a) but for anomalous HRC and anomalous absolute values of 50–200-hPa zonal wind shear.

made to remove fluctuations due to ENSO, the 50–60-day oscillation, etc., from the HRC or tropopause pressure time series). Maps of the coefficients for anomalous HRC correlated with the anomalous strength of the zonal wind shear between 50 and 200 hPa (only winter shown; Fig. 13b) do not correspond as well with the west–east phase HRC spatial patterns of Fig. 5. However, coefficients are very negative (low shear coincident with high HRC values; high shear with low HRC) in most regions and seasons where increased west phase convection is collocated/coincident with a weak QBO influence on tropopause height and favorable west phase shear, such as near northern Australia in winter (cf. Fig. 13b with Figs. 5a, 11a, 12a).

Deep convection influences the height of the tropical tropopause (Reid and Gage 1981; Gage and Reid 1987). Therefore, one cannot discount the possibility that the QBO signal in tropopause height is a result of independent QBO variations in tropical convection. But this seems unlikely considering the theoretical foundation (see section 1) and strong evidence (Fig. 11; Huesmann and Hitchman 2001) for a direct modulation of tropopause height by the QBO, especially because of the evidence for modulation by the QBO far away from the chronically convective regions. However, it does seem plausible that QBO variations of tropopause height could cause QBO variations of deep convection that could then feed back positively on the height variations.

The OLR results generally agree with those for HRC, supporting the idea that the QBO-related variations of OLR are primarily manifestations of deep convection, as opposed to cirrus clouds or other variables affecting OLR. The OLR variations reflect changes in convective cloud amount (cloud frequency and areal extent) and/or height. HRC variations do not reflect cloud height; they are only affected by deep convective cloud amount. However, as discussed in section 1, the QBO variations of HRC are likely to be a result of convective height fluctuations that induce amount variations.

5. Conclusions

Using *Nimbus-6, Nimbus-7,* and *ERBS* data, we assembled a 23-yr OLR record that we believe to be the most consistent OLR record of its length. We partitioned this record and a 17-yr HRC record, both confined to the Tropics, by phase of the QBO. Zonal means for each phase are distinctly different; likewise for seasonal maps. For the most part, the differences indicate diminished convection during the QBO west phase, and enhanced convection during the east phase, especially in regions typically occupied by deep convection. In boreal summer, the relationship is reversed: enhanced west phase convection, diminished east phase convection. Spectral analysis of zonal mean near-equator OLR and HRC reveals significant power at QBO periods. The QBO signal in deep convection appears to be distinct from the ENSO signal, although the brevity of the OLR and HRC records, especially with respect to the ENSO cycle, made it difficult to separate the two signals with

a high degree of certainty. The HRC results indicate that the frequency and/or horizontal extent of convection fluctuates with the QBO. Fluctuations in frequency, horizontal extent, and also cloud height could contribute to the OLR variations.

In parts of the Tropics, the QBO variations of OLR and HRC are physically consistent with QBO variations of the lower-stratospheric to upper-tropospheric zonal wind shear, while in other parts the OLR/HRC and shear variations are physically inconsistent. OLR and HRC correspond much more closely with fluctuations in tropopause height induced by the QBO. OLR and HRC fluctuations do not correspond well with upper-tropospheric vorticity fluctuations associated with the QBO.

The evidence supports the following. In the Tropics, the east phase of the QBO causes the tropopause to be higher than normal, allowing convection to penetrate deeper than normal. The deeper clouds, which tend to have larger diameters than shallower clouds, lead to more convergence of mass, moisture, and energy at low levels, precipitating the formation of more convective clouds; that is, the deeper clouds lead to increased cloud amount. In regions where the QBO effect on tropopause height is weak (at various longitudes, usually away from the equator), strong cross-tropopause zonal wind shear can reduce convection. The entire scenario is reversed during the west phase. Thus, it appears that tropopause height fluctuations may be a primary mechanism through which the QBO influences deep convection, with cross-tropopause shear operating as a secondary mechanism where QBO-induced height fluctuations are small. During boreal summer, a weak QBO influence on tropopause height where most convection is located may allow the shear effect to dominate QBO-related convective behavior in the Tropics.

To address weaknesses in this study, more work must be done to distinguish cirrus from convective variations in the OLR record. Also, a longer HRC record is needed for more definitive results. Furthermore, more work can be done in separating the ENSO signal from the QBO signal in convection. If established, a robust QBO signal in convection would be of great utility for forecasts of tropical rainfall and, considering the fundamental role that tropical convection plays in the global circulation, possibly for forecasts of weather around the globe.

Acknowledgments. The authors are grateful to G. Louis Smith, T. Dale Bess, David Young, Kathy Bush, and Takmeng Wong for their advice and assistance in constructing the NASA OLR record. T. Dale Bess supplied us with the *Nimbus-6* and *Nimbus-7* data. We also thank Fran McLemore for her help with obtaining the *ERBS* data from the NASA Langley Research Center Distributed Active Archive Center. Grace Wahba and Ming Yuan gave us very helpful advice regarding significance tests. This work was supported by National Science Foundation (NSF) Grants ATM-9812429, ATM-0004207 (CC, DM, MH, AH), and ATM-0094416 (DW), and NASA Grant NAG5-11303 (MH, AH). The NCEP reanalyses were obtained from NCAR, which is supported by NSF.

REFERENCES

Bess, T. D., G. L. Smith, and T. P. Charlock, 1989: A ten-year monthly data set of outgoing longwave radiation from Nimbus-6 and Nimbus-7 satellites. *Bull. Amer. Meteor. Soc.,* **70,** 480–489.

Byers, H. R., and R. R. J. Braham, 1949: *The Thunderstorm.* U.S. Government Printing Office, 287 pp.

Chelliah, M., and P. Arkin, 1992: Large-scale interannual variability of monthly outgoing longwave radiation anomalies over the global tropics. *J. Climate,* **5,** 371–389.

Collimore, C. C., M. H. Hitchman, and D. W. Martin, 1998: Is there a quasi-biennial oscillation in tropical deep convection? *Geophys. Res. Lett.,* **25,** 333–336.

Curtis, C., and R. Adler, 2000: ENSO indices based on patterns of satellite-derived precipitation. *J. Climate,* **13,** 2786–2793.

Earth Radiation Budget Experiment Data Management System, 1994: The regional, zonal, and global averages, S-4/S-4N user's guide. NASA Langley Research Center Distributed Active Archive Center, 65 pp.

Gage, K. S., and G. C. Reid, 1987: Longitudinal variations in tropical tropopause properties in relation to tropical convection and El Niño–Southern Oscillation events. *J. Geophys. Res.,* **92,** 14 197–14 203.

Gagin, A., D. Rosenfeld, and R. E. Lopez, 1985: The relationship between height and precipitation characteristics of summertime convective cells in South Florida. *J. Atmos. Sci.,* **42,** 84–94.

Garcia, O., 1985: *Atlas of Highly Reflective Clouds for the Global Tropics: 1971–1983.* U.S. Department of Commerce, 365 pp. [Available from Superintendent of Documents, U.S. Government Printing Office, Washington, DC 20402.]

Gray, W. M., J. D. Scheaffer, and J. A. Knaff, 1992: Influence of the stratospheric QBO on ENSO variability. *J. Meteor. Soc. Japan,* **70,** 975–995.

Grossman, R., and O. Garcia, 1990: The distribution of deep convection over ocean and land during the Asian summer monsoon. *J. Climate,* **3,** 1032–1044.

Gruber, A., and A. F. Krueger, 1984: The status of the NOAA outgoing longwave radiation data set. *Bull. Amer. Meteor. Soc.,* **65,** 958–962.

Hastenrath, S., 1990: The relationship of highly reflective clouds to tropical climate anomalies. *J. Climate,* **3,** 353–365.

Huesmann, A. S., and M. H. Hitchman, 2001: The stratospheric quasi-biennial oscillation in the NCEP reanalyses: Climatological structures. *J. Geophys. Res.,* **106,** 11 859–11 874.

Kalnay, E., and Coauthors, 1996: The NCEP/NCAR 40-Year Reanalysis Project. *Bull. Amer. Meteor. Soc.,* **77,** 437–471.

Kilonsky, B., and C. S. Ramage, 1976: A technique for estimating tropical open-ocean rainfall from satellite observations. *J. Appl. Meteor.,* **15,** 972–975.

Kistler, R., and Coauthors, 2001: The NCEP–NCAR 50-year reanalysis: Monthly means CD-ROM and documentation. *Bull. Amer. Meteor. Soc.,* **82,** 247–267.

Knaff, J. A., 1993: Evidence of a stratospheric QBO modulation of tropical convection. Dept. of Atmospheric Science, Colorado State University, Fort Collins, CO, Paper 520, 91 pp.

Knox, J. A., 1997: Generalized nonlinear balance criteria and inertial stability. *J. Atmos. Sci.,* **54,** 967–985.

Kyle, H. L., P. E. Ardanuy, and R. R. Hucek, 1986: *El Niño and Outgoing Longwave Radiation: An Atlas of Nimbus-7 Earth Radiation Budget Observations.* NASA Reference Publ. 1163, 98 pp.

Lucas, L. E., D. E. Waliser, P. Xie, J. E. Janowiak, and B. Liebmann, 2001: Estimating the satellite equatorial crossing time biases in the daily, global outgoing longwave radiation dataset. *J. Climate,* **14,** 2583–2605.

Mapes, B. E., 1993: Gregarious tropical convection. *J. Atmos. Sci.,* **50,** 2026–2037.

Mecikalski, J. R., and G. J. Tripoli, 2003: Influence of upper tropospheric inertial stability on the convective transport of momentum. *Quart. J. Roy. Meteor. Soc.,* in press.

Montgomery, M. T., and B. F. Farrell, 1993: Tropical cyclone formation. *J. Atmos. Sci.,* **50,** 285–310.

Plumb, R. A., and R. C. Bell, 1982: A model of the quasi-biennial oscillation on an equatorial beta-plane. *Quart. J. Roy. Meteor. Soc.,* **108,** 335–352.

Randel, W. J., F. Wu, and D. J. Gaffen, 2000: Interannual variability of the tropical tropopause derived from radiosonde data and NCEP reanalyses. *J. Geophys. Res.,* **105,** 15 509–15 523.

Reid, G. C., and K. S. Gage, 1981: On the annual variation in height of the tropical tropopause. *J. Atmos. Sci.,* **38,** 1928–1938.

——, and ——, 1985: Interannual variations in the height of the tropical tropopause. *J. Geophys. Res.,* **90,** 5629–5635.

Rosenfeld, D., and A. Gagin, 1989: Factors governing the total rainfall yield from continental convective clouds. *J. Appl. Meteor.,* **28,** 1015–1030.

Trepte, C. R., 1993: Tracer transport in the lower stratosphere. Ph.D. dissertation, University of Wisconsin—Madison, 169 pp.

Tung, K. K., and H. Yang, 1994: Global QBO in circulation and ozone. Part I: Reexamination of observational evidence. *J. Atmos. Sci.,* **51,** 2699–2707.

Ulanski, S. L., and M. Garstang, 1978: The role of surface divergence and vorticity in the life cycle of convective rainfall. Part I: Observation and analysis. *J. Atmos. Sci.,* **35,** 1047–1062.

Waliser, D. E., and W. Zhou, 1997: Removing satellite equatorial crossing time biases from the OLR and HRC datasets. *J. Climate,* **10,** 2125–2146.

——, N. E. Graham, and C. Gautier, 1993: Comparison of the highly reflective cloud and outgoing longwave radiation datasets for use in estimating tropical deep convection. *J. Climate,* **6,** 331–353.

Wallace, J. M., E. M. Rasmusson, T. P. Mitchell, V. E. Kousky, E. S. Sarachik, and H. von Storch, 1998: On the structure and evolution of ENSO-related climate variability in the tropical Pacific: Lessons from TOGA. *J. Geophys. Res.,* **103,** 14 241–14 259.

Wang, B., 1994: Climatic regimes of tropical convection and rainfall. *J. Climate,* **7,** 1109–1118.